CSIRO PUBLISHING

Australian Journal of Physics

Volume 53, 2000

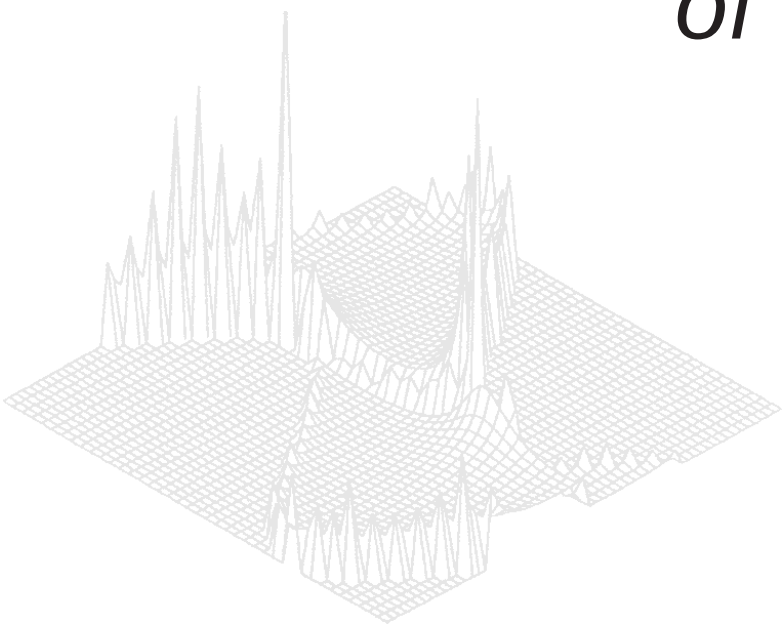

A journal for the publication of
original research in all branches of physics

www.publish.csiro.au/journals/ajp

All enquiries and manuscripts should be directed to
Australian Journal of Physics
CSIRO PUBLISHING
PO Box 1139 (150 Oxford St)
Collingwood Telephone: 61 3 9662 7626
Vic. 3066 Facsimile: 61 3 9662 7611
Australia Email: peter.robertson@publish.csiro.au

Published by **CSIRO** PUBLISHING
for CSIRO and
the Australian Academy of Science

Aust. J. Phys., 2000, **53**, 835–850

The Didjeridu: Lip Motion and Low Frequency Harmonic Generation

Lloyd C. L. Hollenberg

School of Physics, University of Melbourne,
Vic. 3010, Australia.

Abstract

The dynamic acoustics of the Australian didjeridu are studied by separately considering transverse and longitudinal lip vibration models in the context of highly non-sinusoidal lip motion. Time-domain computer simulations are performed based on these lip models coupled to the input impedance function of a straight pipe. For the purposes of direct comparison, detailed results are reported here for lip motion leading to both sinusoidal lip opening area functions (characteristic of higher frequency brass instruments) and the more complex non-sinusoidal (approximately half-closed cycle) case characteristic of the didjeridu. Over a range of lip resonance frequencies, the sounding frequency for the transverse (longitudinal) model is found to be below (above) both the lip and fundamental pipe resonance frequencies, in qualitative agreement with linear theory for these value types. A striking difference is found between the two models when comparing the effect of significant lip closure in the non-sinusoidal cycle—the sounding frequency in the transverse case is raised by up to 10%, whilst essentially unaltered in the longitudinal model. The effect the lips sticking during the non-sinusoidal cycle was considered by increasing the damping force upon closure, and was found in both transverse and longitudinal models to weaken significantly the generation of harmonics in the sound.

1. Introduction

The Australian *yidaki*, commonly known as the *didjeridu*, is an ancient wind instrument originating from the northern regions of the continent. The didjeridu is made from a slender tree trunk or branch, initially hollowed out by white ants. Subsequent finishing of the instrument by boring out the dead wood and thinning the walls produces a tube of length 1–1.5 m with varying taper. The small end usually has a diameter of about 3–5 cm and, with no modification other than a ring of beeswax or resin for player comfort, serves as the mouthpiece of the instrument.

To play the didjeridu one buzzes the lips, with the appropriate tension, to sound a low drone, which is usually blown continuously by the technique of circular breathing. Obtaining just this basic drone note is a matter of considerable control: the unskilled will most likely produce a 'blurting' note. Careful adjustment of the lip position and tension must be made until the cleaner sound of the drone is triggered.

The natural breathing cycle, and movement/position of the cheeks, jaw and tongue are used to produce percussive rhythms and great variation in the timbre of the sound. Vocalisation is also added to great effect: oftentimes mimicking the sounds of animals reverberating in a background of the rhythmic drone. Excitations of individual resonances above the fundamental, known as 'overblown notes' (similar in sound to a horn), are occasionally used to punctuate the sound. It is quite striking the degree to which the physical simplicity of the instrument belies its potential for highly developed music. In fact, in ethno-musicological terms the didjeridu is unique in that the music developed on it by the

 10.1071/PH00100 0004-9506/00/060835$05.00

indigenous people of Australia, without any technological improvements, has considerably greater complexity to that produced on similar wind instruments by any other culture (Jones 1967).

The didjeridu has become popular worldwide, however, it is only recently that the study of the acoustics of this instrument has received any attention. The technical works to date are the pioneering theoretical treatment of Fletcher (1983, 1996) and the measurements of lip motion and input impedance carried out by Wiggins (1985). A frequency spectrum of the sound is given in Fig. 1, for the case of the drone note with minimal formant production, and shows the basic structure of dominant odd harmonics (roughly corresponding in frequency to the resonances of the pipe), interspersed with suppressed even harmonics. Vocal tract resonances, at around 1500 Hz and higher, can be manipulated by the player in both frequency and strength.

While the passive acoustics of the didjeridu pipe (straight and flared) are well described (Fletcher 1983, 1996), there does not yet exist a quantitative analysis of the generation of sound in this instrument as has been carried out for various Western wind instruments. The dynamic acoustics of this instrument remain unexplored. Given the origin of the instrument itself and the complexity of the playing style, it perhaps comes as no surprise that the dynamic acoustics are far more interesting than a simple valve driven oscillating column of air. For the sake of clarity we can break the acoustic system down into four main components—didjeridu pipe, lip-valve, vocal tract cavity and vocal folds.

The first part of this system to consider is the didjeridu itself. Unlike most Western instruments, there is no standard to which the didjeridu is traditionally made, although the pipe can be tuned to a particular fundamental pitch by cutting to the appropriate length. Natural

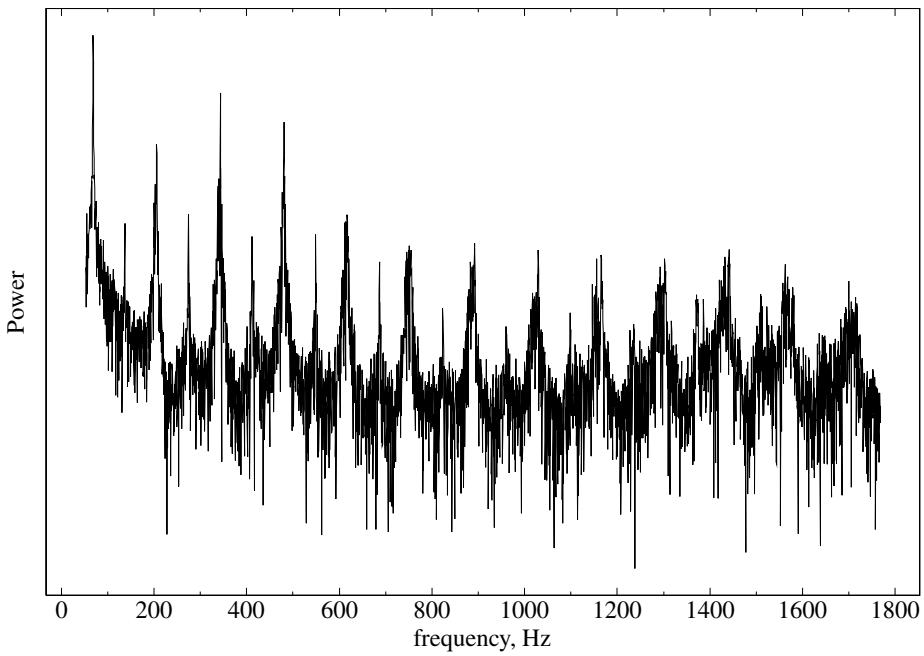

Fig. 1. Low frequency spectrum measured during the sounding of the drone note on a 1250 mm pipe (radius 20 mm).

variations in the degree of conical flare, bore smoothness, and curvature all contribute to the uniqueness of each instrument. Fortunately for our purposes, these unpredictable and complex characteristics, which would be extremely difficult to model, have a relatively small effect; for example, one can obtain an authentic sound (at least indistinguishable to the untrained ear) from a length of plastic pipe. This of course reflects the fact that the acoustic impedance of the didjeridu is well approximated by that of a smooth bore pipe (possibly flared) and is well understood; for this reason (and the added simplicity of the absence of a mouthpiece) the didjeridu may hold an important place in computer simulation of lip-driven wind instruments. In these preliminary investigations we will model the didjeridu itself as a straight pipe.

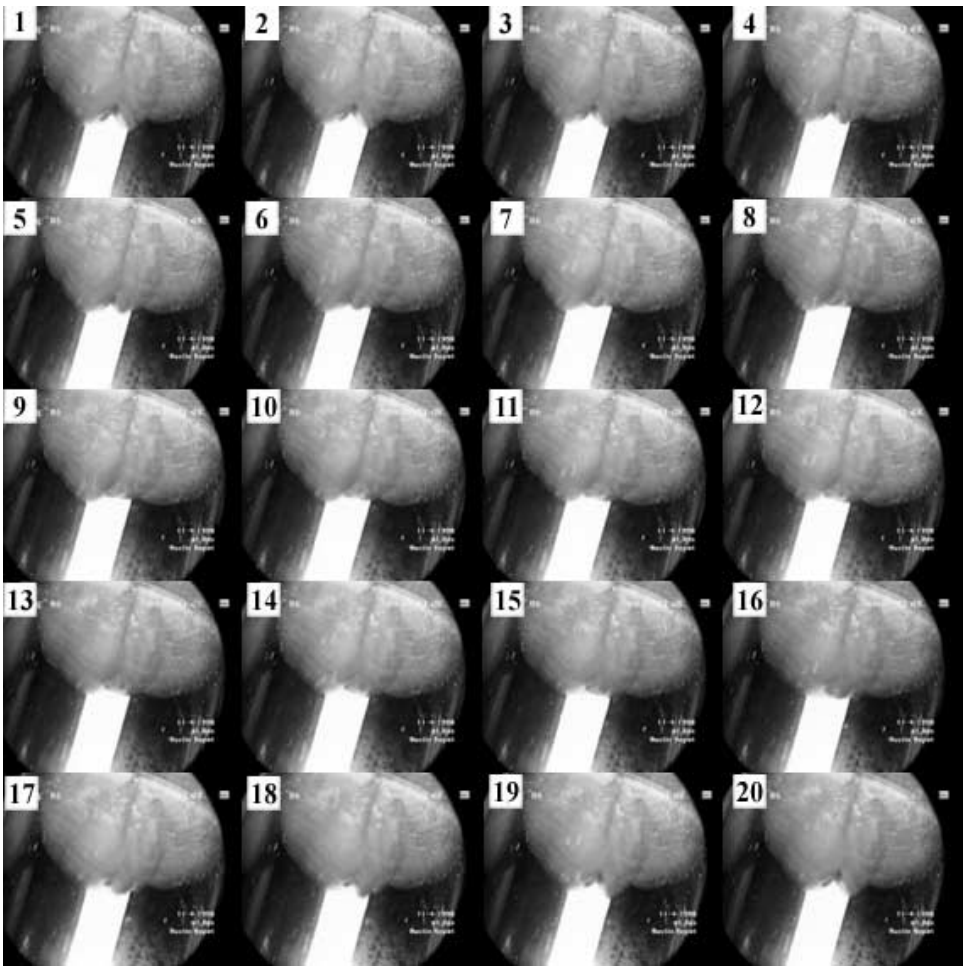

Fig. 2. Strobe measurement sequence showing (semi side-on view) one cycle of the lip motion during the sounding of the drone note on a 1000 mm pipe (85 Hz fundamental, radius 20 mm). Frames 1 and 20 correspond to maximum lip opening. For calibration, the bright strip in each frame is 10 mm wide. [Strobe measurements taken in collaboration with J. Oates.]

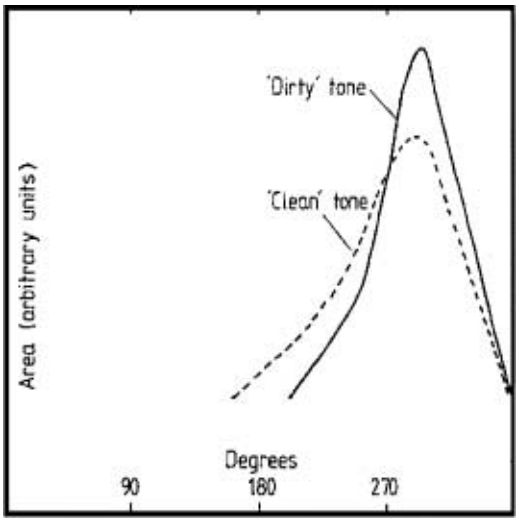

Fig. 3. Wiggins' lip area analysis showing the half-closed cycle [reproduced from Wiggins (1985)].

It is well known that the biomechanical modelling of the vocal tract and vocal folds is a considerable challenge in its own right, let alone in conjunction with the valve/air-column system. However, it also turns out that the coupling between the didjeridu pipe and the lip valve is quite unusual and more complex, compared with other lip-driven instruments. A stroboscopic study of the lip motion carried out by Wiggins shows a very interesting, highly non-sinusoidal lip motion where the lips actually stay closed on contact for a relatively long time—up to half the cycle. Independent observations shown in Fig. 2 confirm these long closure times. The summary of the analysis of lip opening areas carried out by Wiggins is reproduced in Fig. 3. Such complexity of lip motion is perhaps not too surprising in this context as it is reminiscent of low frequency vocal-fold motion. In no other dynamical treatment of lip- or reed-driven wind instruments has such an extreme cycle been taken into account.

Before all components of the didjeridu can be modelled in unison, a major undertaking, we first seek an understanding of the effect of the unusual lip motion on the harmonic generation in the valve/air-column system. To this extent, the work presented here represents a first attempt at understanding the dynamic acoustics of the didjeridu, by time-domain simulation. Both longitudinal and transverse models of lip motion are considered in the regime of non-sinusoidal oscillation—the (approximately) half-closed cycle. In the context of whether brass players' lips are best modelled by a transverse or longitudinal 'reed', there are relevant works by Yoshikawa (1995), who carried out an experimental study of the type of lip motion supported with and without a mouthpiece for varying frequencies, and Chen and Weinreich (1996) who concurred with Yoshikawa's findings (in the frequency range 200–350 Hz) that human lips function mainly as 'outward striking' reeds. In the case of the didjeridu the frequencies involved are much lower (the longest pipe length in Yoshikawa's work was 400 mm), and it is not at all clear that these conclusions hold given the non-sinusoidal motion of the lips. In this work the components of lip motion in the transverse and longitudinal directions are considered separately in order to avoid the proliferation of parameters in a two-dimensional, multi-mass lip model. Such complexities can be introduced at a later stage with the guidance of quantitative strobe measurements.

Given a specific lip model, the changing character of harmonic generation in the non-sinusoidal regime is studied for various lip parameters. Furthermore, the case of sinusoidal oscillation is also considered in order to directly ascertain the differences between the non-sinusoidal didjeridu regime and the typical lip motion used in trumpet simulations (Adachi and Sato 1995, 1996). The differences between harmonic generation in longitudinal and transverse models also turns out to be quite significant, perhaps indicating their relative importance in a more complex combined model.

The paper is set out as follows. In Section 2 a brief review is presented of the time-domain formalism connecting pressure and volume flow through the input impedance and reflection function. Section 3 deals with the two lip models in the context of the didjeridu model. A short discussion of the numeric aspects of the simulation is given in Section 4, and the results discussed in Section 5. Conclusions are presented in Section 6.

2. Input Impedance and Reflection Function

To begin the treatment of the didjeridu, we first note that we are primarily interested in calculating the pressure and volume flow at the mouth end of the pipe as a function of time ($p(t)$ and $U(t)$ respectively). In the frequency domain these quantities are related simply by the acoustic input impedance $Z(\omega)$ ($\omega = 2\pi f$). However, as the lip dynamics are (so far) most conveniently modelled in the time domain, the relationship between pressure and volume at the mouthpiece is more complicated, requiring lengthy calculation of the Green function. Schumacher (1981) developed a technically simpler approach using the reflection function $r(t)$, for which $p(t)$ and $U(t)$ are related by the integral equation

$$p(t) = Z_0 U(t) + \int_0^\infty r(t')[Z_0 U(t-t') + p(t-t')]\,dt', \tag{1}$$

where

$$r(t) \equiv \frac{1}{2\pi}\int_{-\infty}^{\infty} \frac{Z(\omega) - Z_0}{Z(\omega) + Z_0} \mathrm{e}^{j\omega t}\,d\omega. \tag{2}$$

The characteristic impedance of a pipe of radius a is $Z_0 = \rho c/\pi a^2$, where ρ and c are the density of air and the speed of sound respectively. The input impedance $Z(\omega)$ of the didjeridu (assuming only plane wave propagation), at angular frequency $\omega = 2\pi f$, can be written down analytically. In the idealised case of zero load impedance at the open end and no propagation losses, the input impedance of a cylindrical pipe of physical length L_0, and hence the acoustic length $L = L_0 + 0.61a$, is

$$Z_{\text{ideal}}(\omega) = jZ_0 \tan\frac{\omega L}{c}. \tag{3}$$

This simple approximation provides a guide to the form of the reflection function which in this case can be calculated exactly to give a delta function return spike:

$$r_{\text{ideal}}(t) = -\delta(t - 2L/c). \tag{4}$$

It is possible to calculate a more physically relevant reflection function which includes thermal and viscous losses and radiation corrections at the open end; the input impedance in this case is given by (Pratt *et al.* 1977)

$$Z(\omega) = Z_0 \frac{\tanh\alpha(\omega) + j\tan\beta(\omega)}{1 + j\tanh\alpha(\omega)\tan\beta(\omega)}, \tag{5}$$

where

$$\alpha(\omega) = \frac{L}{ca}\sqrt{\frac{\omega}{2\rho}}\left[\sqrt{\eta} + (\gamma - 1)\sqrt{\frac{\kappa}{C_P}}\right] + \left[\frac{\beta(\omega)a}{2}\right]^2,$$

$$\beta(\omega) = \frac{\omega L}{c}, \tag{6}$$

and the various constants are

ρ = density of air,
η = coefficient of shear viscosity of air,
κ = thermal conductivity of air,
C_P = specific heat of air at constant pressure,
γ = ratio of specific heats for air.

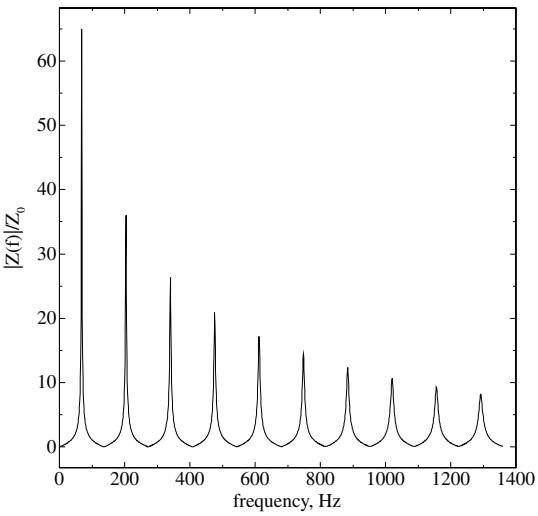

Fig. 4. Theoretical input impedance curve $Z(\omega)$ relative to the characteristic impedance Z_0 for a straight pipe of length 1250 mm and radius 20 mm. The fundamental frequency occurs in this case at 68 Hz.

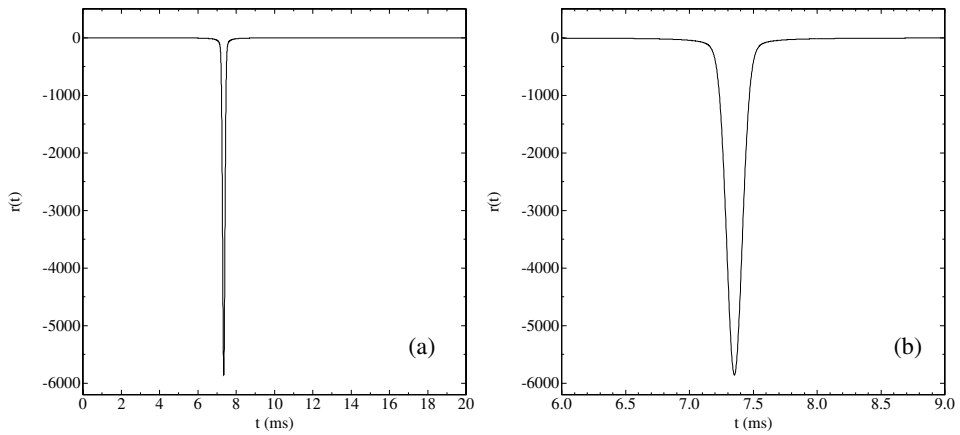

Fig. 5. (a) Calculated reflection function $r(t)$ based on the input impedance $Z(\omega)$ for a straight pipe of length 1250 mm and radius 20 mm. (b) An enlarged view of the return spike in Fig. 5*a*.

The reflection function can be calculated numerically to high accuracy by careful quadrature of equation (2). For the choice of tube parameters used here ($L_0 = 1250\,\text{mm}$ and $a = 20\,\text{mm}$) the input impedance and reflection function are plotted in Figs 4 and 5 respectively (all calculations were carried out at $T = 20°\text{C}$). Since we are restricting ourselves to a straight pipe the maxima in $|Z(\omega)|$ correspond to the resonant frequencies at odd multiples of the fundamental, $f_1 = c/4L$ (68 Hz in this case). The return spike of the reflection function at $t = 2L/c$ is more spread out than $r_{\text{ideal}}(t)$ due to radiation corrections and propagation losses.

3. Lip Vibration Models and Airflow Dynamics

The formalism we use to model the lip dynamics is based to a large extent, albeit with several differences, to that developed by Adachi and Sato (1995) for the trumpet. The basic geometry of the didjeridu model is shown in Fig. 6. The pressure inside the mouth cavity p_0 is assumed to be static, while the average pressure on the surface of the lip opening $p_{\text{lip}}(t)$ and at the mouthpiece of the didjeridu ($x = 0$) $p(t)$ vary with time. In any future study which includes vocal tract resonances the pressure in the mouth cavity will no longer be static. Given the symmetry of the instrument we have so far assumed the airflow in the pipe can be treated as one dimensional. Around the lips, this is a more drastic approximation, but allows one to relate pressure and volume flow analytically, rather than attempting to solve the three-dimensional Navier–Stokes problem. We thus follow the standard reduction to one-dimensional flow.

In region I the air undergoes contraction, while remaining laminar, so that energy and momentum are conserved. In the expansion in region II the flow has a large Reynold's number and forms a jet, conserving only momentum and dissipating energy as heat. The one-dimensional reduction gives the following non-linear equations for the pressures and

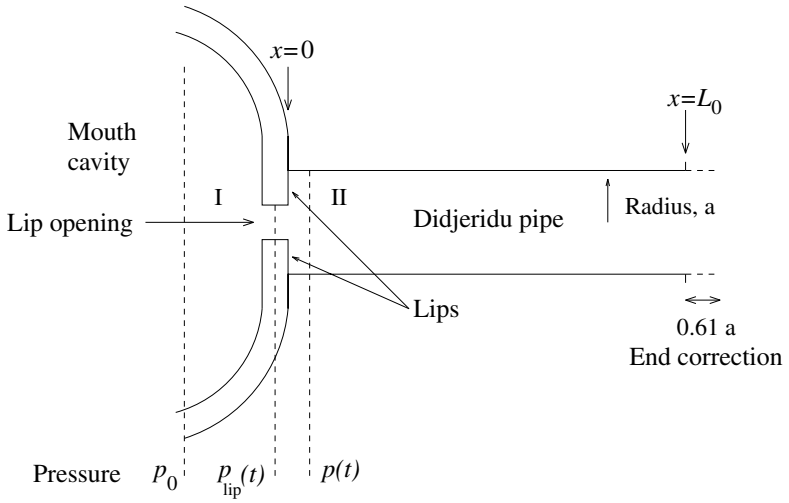

Fig. 6. Schematic of the side view of the didjeridu and lip opening, defining the blowing pressure p_0, and pressures at the mouthpiece and lip $p(t)$ and $p_{\text{lip}}(t)$ respectively.

volume flow (Adachi and Sato 1995):

$$p_0 - p_{\text{lip}}(t) = \frac{\rho}{2}\left[\frac{U(t)}{A_{\text{lip}}(t)}\right]^2 + \frac{\rho d}{A_{\text{lip}}(t)}\frac{\partial U(t)}{\partial t}, \tag{7}$$

$$p_{\text{lip}}(t) - p(t) = \rho U(t)^2\left[\frac{A_{\text{lip}}(t) - A_{\text{D}}}{A_{\text{D}}^2 A_{\text{lip}}(t)}\right], \tag{8}$$

where $A_{\text{lip}}(t)$ is the time dependent area of the lip opening, $A_{\text{D}} = \pi a^2$ (the cross sectional area of the didjeridu) and d is the lip thickness. These equations will be used in conjunction with the reflection function integral equation to determine the pressure $p(t)$ and the volume flow $U(t)$.

The one-dimensional lip vibration models (Adachi and Sato 1995) separately describe transverse and longitudinal motion. For both models the lip opening is rectangular with breadth b: the upper and lower lips are geometrically identical and move symmetrically.

In the transverse 'sliding door' model (see Fig. 7*a*), the dynamical variable is the displacement $y(t)$ and is governed by the equation (the superscript 'T' denotes the transverse case)

$$m\frac{d^2y(t)}{dt^2} = F^{\text{T}}_{\text{damping}} + F^{\text{T}}_{\text{Bernoulli}} + F^{\text{T}}_{\text{restore}} + F^{\text{T}}_{\text{closure}}, \tag{9}$$

where

$$\begin{aligned} F^{\text{T}}_{\text{damping}} &= -\frac{\sqrt{mk}}{Q}\,dy(t)/dt, \\ F^{\text{T}}_{\text{Bernoulli}} &= dbp_{\text{lip}}(t), \\ F^{\text{T}}_{\text{restore}} &= -k(y(t) - y_0), \\ F^{\text{T}}_{\text{closure}} &= -k_{\text{cl}}y(t), \quad \text{for } y(t) < 0. \end{aligned}$$

In the above expressions m is the lip mass, k the spring stiffness, Q the quality factor, b the lip breadth and y_0 the equilibrium displacement. The closure force acts only when the lips touch. The lip displacement $y(t)$ is coupled to the pressure and volume flow equations through $p_{\text{lip}}(t)$ and the area of the lip opening

$$A^{\text{T}}_{\text{lip}}(t) = 2by(t). \tag{10}$$

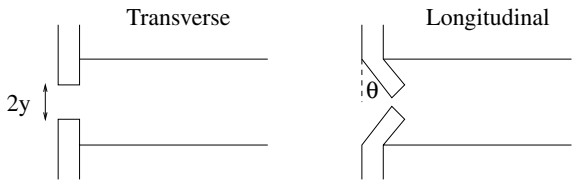

a) Sliding Door b) Swinging Door

Fig. 7. One-dimensional lip models representing transverse and longitudinal motion.

In the longitudinal 'swinging door' model (Fig. 7*b*), the equation of motion for the lip angle $\theta(t)$ is (the superscript 'L' denotes the longitudinal case)

$$ml\frac{d^2\theta(t)}{dt^2} = F^{\mathrm{L}}_{\mathrm{damping}} + F^{\mathrm{L}}_{\mathrm{pressure}} + F^{\mathrm{L}}_{\mathrm{Bernoulli}} + F^{\mathrm{L}}_{\mathrm{restore}} + F^{\mathrm{L}}_{\mathrm{closure}}, \tag{11}$$

where

$$\begin{aligned} F^{\mathrm{L}}_{\mathrm{damping}} &= -\frac{l\sqrt{mk}}{Q}\, d\theta(t)/dt, \\ F^{\mathrm{L}}_{\mathrm{pressure}} &= \tfrac{1}{2}bl(p_0 - p(t)), \\ F^{\mathrm{L}}_{\mathrm{Bernoulli}} &= dbp_{\mathrm{lip}}(t)\sin\theta(t), \\ F^{\mathrm{L}}_{\mathrm{restore}} &= -kl(\theta(t) - \theta_0), \\ F^{\mathrm{L}}_{\mathrm{closure}} &= -k_{\mathrm{cl}}l(\theta(t) - \theta_{\mathrm{cl}}), \quad \text{for } \theta(t) < \theta_{\mathrm{cl}}, \end{aligned}$$

where l is the lip length, θ_0 the equilibrium angle and θ_{cl} the closure angle. The time dependent lip opening area function is

$$A^{\mathrm{L}}_{\mathrm{lip}}(t) = 2bl(\cos\theta_{\mathrm{cl}} - \cos\theta(t)). \tag{12}$$

For the swinging door model an extra term, $bl^2 d\theta(t)/dt$ corresponding to the air swept out by the lips, must be added to the volume flow.

4. Numerics

For a given set of parameters we are interested primarily in solving for the functions $p(t)$ and $U(t)$, and thus the lip area $A_{\mathrm{lip}}(t)$ over a sequence of time steps. At a given time step t_n the ODEs for the lip dynamical variables are solved to give $y(t_n)$ or $\theta(t_n)$ (depending on the model) and hence the lip area $A_{\mathrm{lip}}(t_n)$. A relation between $p(t_n)$ and $U(t_n)$ is obtained by eliminating the lip pressure $p_{\mathrm{lip}}(t)$ from the non-linear airflow equations (7) and (8). When combined with the discretised integral equation (1) we finally obtain a quadratic in $U(t_n)$, from which the solutions for $p(t_n)$ and $p_{\mathrm{lip}}(t_n)$ follow.

A potentially time consuming aspect of the numerical solution is the quadrature required in the calculation of the reflection function $r(t)$. This is a crucial step in the calculation as all the information about the pipe resonances are encapsulated in $r(t)$ through the input impedance $Z(\omega)$. Since we have chosen a particular set of pipe parameters (e.g. the length and radius of the pipe was held fixed), it is far more efficient to calculate $r(t_n)$ at each time step to high accuracy once beforehand and read the array from disk at the start of each simulation. It was explicitly demonstrated that the quadrature precision in $r(t_n)$ had a negligible effect on the final calculations.

Initial runs exploring the parameter space were made at a sampling rate of 125 kHz over 400 ms. All data shown here are for a sampling rate of 250 kHz over 1000 ms. Appreciable differences in the results for the two step sizes occurred only in the case of unusual, and relatively rare, oscillation regimes (i.e. unstable or chaotic oscillation); the results shown here are stable with respect to step size.

Table 1. Predetermined model parameter values used in all simulations

Parameter	Value
Tube length L_0	1250 mm
Tube radius a	20 mm
Lip breadth b	10 mm
Lip thickness d	3 mm
Quality factor Q	5
Closing angle (L model) θ_{cl}	40°

5. Results and Discussion

In each of the models we consider there is a large number of parameters, typical of a biomechanical problem. In Table 1 we list the non-varying parameters values used in the simulations. The fundamental frequency of our theoretical pipe is 68 Hz—the same as for the data in Fig. 1. From the initial strobe measurements study it became clear that between players there are considerable variations in basic lip geometry, symmetry, and motion, so the values used are representative only. For the same reason only symmetric lip model geometries are considered.

Following Adachi and Sato we assume the vibrating lip mass m is inversely proportional to the lip resonance frequency f_{lip}. That is, we write $m \equiv \lambda/4\pi^2 f_{\mathrm{lip}}$, which accordingly gives a spring constant $k = \lambda f_{\mathrm{lip}}$. The introduced parameter λ is then used to control the spring constant (or stiffness), while at the same time maintaining a frequency dependence in the mass. Here, consistency is maintained by adjusting the lip geometry such that the geometrical mass is the same as the vibrating mass, i.e. for a constant lip breadth b and thickness d, the lip length l is adjusted for a given λ so that $m = bdl\rho_{\mathrm{lip}}$ (typically l is of order 3–8 mm). Thus, the parameters that are used here to control the intrinsic lip dynamics are f_{lip} and λ. Presumably, the player has some control over lip tension and hence the parameter f_{lip}, so it is of interest to study how the final sounding frequency varies with the lip resonance frequency.

In adjusting the various model parameters we aim to achieve a lip motion with a sensible area function, $A_{\mathrm{lip}}(t)$. We can broadly define two regimes of lip oscillation: a sinusoidal area function (where the lips just barely touch), and non-sinusoidal area function (where the lips stay closed for a significant fraction of the cycle). The stroboscopic measurements indicate a motion where the lips actually stick together, while still in combined motion, and close for an appreciable time—for 50% of the cycle or more.

Such a half-closed cycle is very different to that in other lip-driven instruments, such as the trumpet, sounding for the most part at higher frequencies. In order to be able to make a direct comparison of the effect of such large closure times on harmonic generation we consider both types of oscillations. Furthermore, we omit the closure force, which in the trumpet simulations was added with an arbitrary spring constant of $k_{\mathrm{cl}} = 3k$. For the sinusoidal case the closure force is in fact negligible because the relative time that the lips are closed is short and the magnitude of the closure force induced is very small. On the other hand, the non-sinusoidal cycle occurs in this low frequency regime precisely because the lips stick on contact, which is opposite to the closure force defined in the trumpet simulations. In the non-sinusoidal simulations the effect of such a 'sticking' force is also considered.

(5a) Sinusoidal Lip Area Function

Detailed simulation results for typical sinusoidal area functions are shown in Figs 8 and 9 for the transverse and longitudinal models respectively. In order to avoid unusually large lip area openings (i.e. $> 100\,\mathrm{mm}^2$), a lower blowing pressure was required in the transverse model compared to that in the longitudinal model. Typical lip area openings, as observed by Wiggins, were achieved using static mouth pressure values of $p_0 = 1.2\,\mathrm{kPa}$ and 2.0 kPa in the transverse and longitudinal models respectively. The basic strategy for simulation in either model was as follows: for a given lip resonance frequency, spring constant, lip geometry (i.e. length, breadth and thickness) and blowing pressure, the equilibrium position (θ_0 or y_0) was adjusted until the desired cycle was obtained (i.e. in the sinusoidal case the lips touch for a minimal fraction of the cycle) as a steady state. Typically, the system took about 50–100 ms to settle down to its cyclic steady state behaviour.

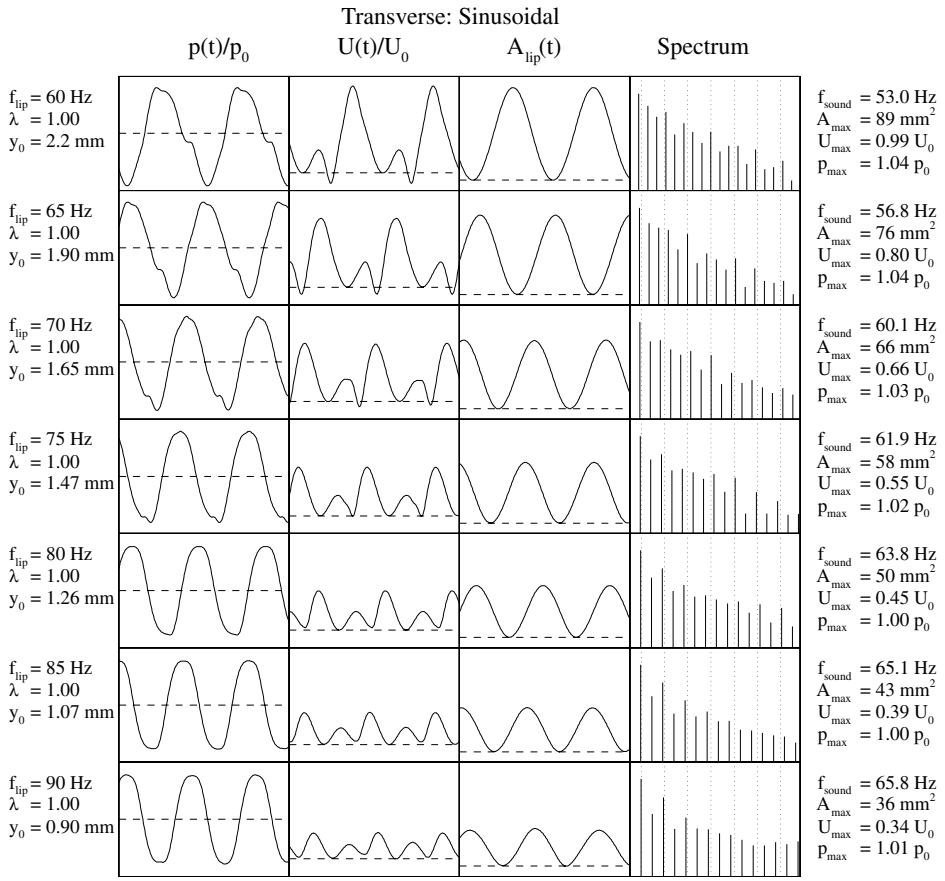

Fig. 8. Sinusoidal lip-motion simulation results (960 to 1000 ms): transverse model ($p_0 = 1.2\,\mathrm{kPa}$). For each quantity, the plot scales are all the same (maximum values of the data set given as a guide). The horizontal dashed lines indicate unity in the case of $p(t)/p_0$ and zero otherwise. The log plots (base 10) of the power spectra shown for the pressure wave all have the same scale: ranging from -11 to $+2$. Resonance frequencies of the pipe are shown as vertical dotted lines.

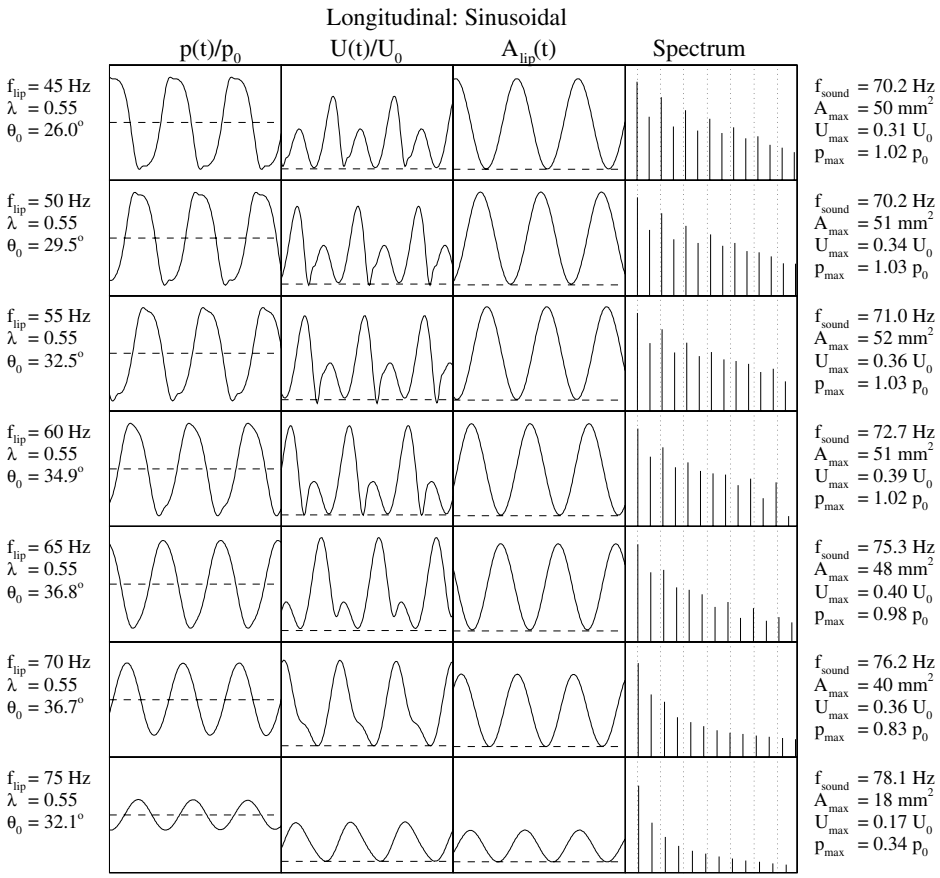

Fig. 9. Sinusoidal lip-motion simulation results (960 to 1000 ms): longitudinal model ($p_0 = 2.0$ kPa). For each quantity, the plot scales are all the same (maximum values of the data set given as a guide). The horizontal dashed line indicates unity in the case of $p(t)/p_0$ and zero otherwise. The log plots (base 10) of the power spectra shown for the pressure wave all have the same scale: ranging from -11 to $+2$. Resonance frequencies of the pipe are shown as vertical dotted lines.

In broad terms the results in this low frequency regime compare well with the analogous simulations carried out for the trumpet. It appears that the steady state condition in the longitudinal case can be supported with relatively low lip resonance frequencies f_{lip}—in the case shown down to at least 45 Hz. The sounding frequency f_{sound} in the longitudinal case is correspondingly much higher than f_{lip}, especially at low frequency (see Fig. 12). In contrast, the transverse model has the opposite behaviour—relatively high lip resonance frequencies, with $f_{\text{sound}} < f_{\text{lip}}$ in general. The lip resonance frequencies shown approximately define the operating limits of the two models for the set of parameters in Table 1.

The relative magnitude of f_{sound} and f_{lip} in both models agrees with the predictions of linear theory (Fletcher 1993; Adachi and Sato 1995) where the longitudinal valve $(+, -)$ acts as a generator only above the resonance frequency of the pipe and valve resonance frequency, while the transverse valve $(+, +)$ acts only below these two frequency limits.

Harmonic generation in a lip-driven instrument occurs due to the non-linear airflow around the lips, in tandem with the natural resonances of the linear acoustic device

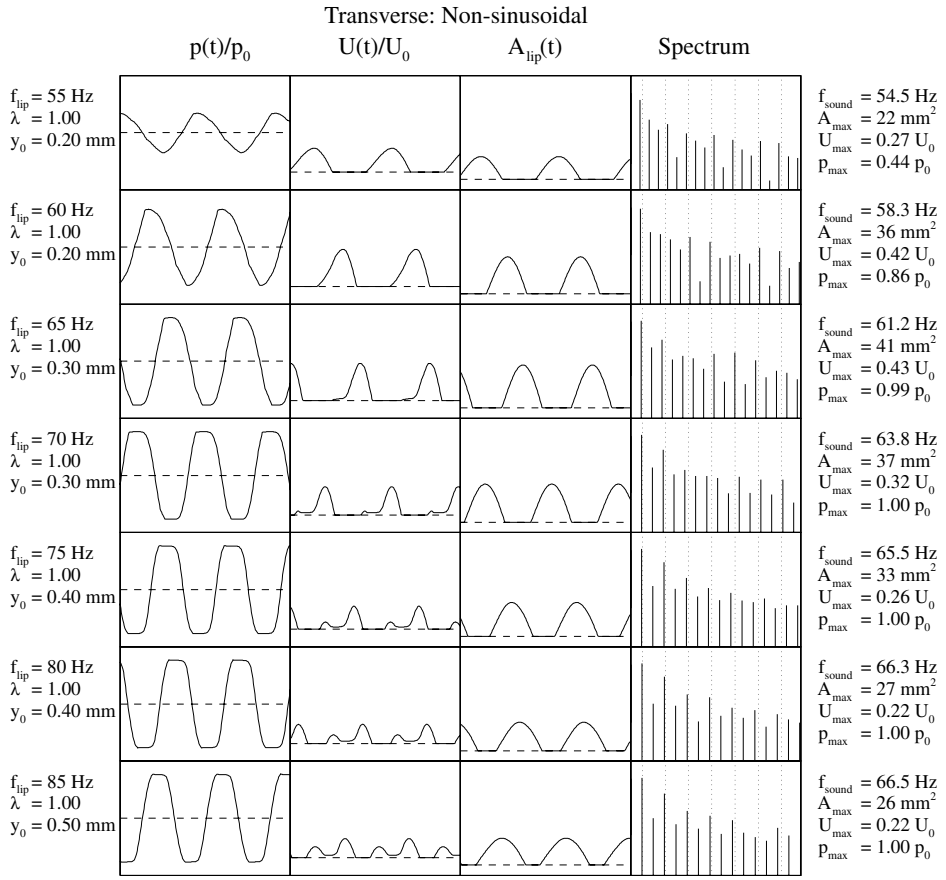

Fig. 10. Non-sinusoidal lip-motion simulation results (960 to 1000 ms): transverse model ($p_0 = 1.2$ kPa) with significant closure fractions (30% to 40%). For each quantity, the plot scales are all the same (maximum values of the data set given as a guide). The horizontal dashed line indicates unity in the case of $p(t)/p_0$ and zero otherwise. The log plots (base 10) of the power spectra shown for the pressure wave all have the same scale: ranging from -11 to $+2$. Resonance frequencies of the pipe are shown as vertical dotted lines.

(the maxima in the input impedance). The details of harmonic generation will depend on the dynamics of the lips and the resulting non-linear airflow. For the case of the straight pipe didjeridu, one would expect the odd harmonics, corresponding to the maxima of the input impedance, to dominate, however, in the actual spectra (see Fig. 1) one also finds the generation of even harmonics which is stronger than the theoretical input impedance curves would suggest, but still significantly weaker than the odd harmonics. It is interesting to note that, in general, the generation of even harmonics is stronger in the transverse model, and the variation with model parameters of the character of harmonic generation is greater.

(5b) Non-sinusoidal Lip Area Function

Within the one-dimensional models considered here, the relatively large closure times required for the half-closed cycle, together with the combined motion upon closure, can be achieved by allowing the lips to pass through each other, with non-zero velocity during

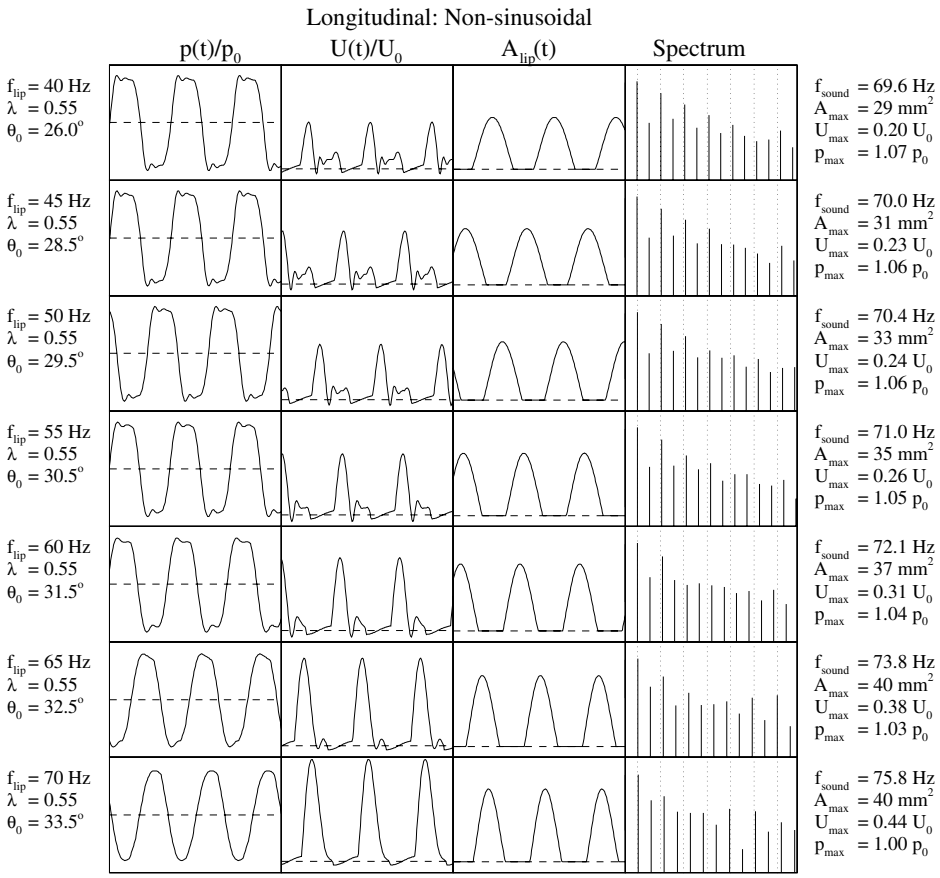

Fig. 11. Non-sinusoidal lip-motion simulation results (960 to 1000 ms): longitudinal model ($p_0 =$ 1.2 kPa) with significant closure fractions (30% to 40%). For each quantity, the plot scales are all the same (maximum values of the data set given as a guide). The horizontal dashed line indicates unity in the case of $p(t)/p_0$ and zero otherwise. The log plots (base 10) of the power spectra shown for the pressure wave all have the same scale: ranging from -11 to $+2$. Resonance frequencies of the pipe are shown as vertical dotted lines.

closure. The equilibrium position in both models was adjusted until an approximately half-closed cycle was obtained. The detailed results for these simulations are shown in Figs 10 and 11 for the transverse and longitudinal models respectively. Typically, the closure fractions shown (around 40% of the cycle) represent the maximum one could achieve and still maintain a steady state motion. The summary of sounding frequency versus lip resonance frequency is given in Fig. 12 in conjunction with the sinusoidal cycle results.

In the non-sinusoidal cycle one obtains, perhaps not surprisingly, a more complex pressure and volume flow waveform. The third harmonic in particular seems to be slightly enhanced and there is a clearer suppression of even harmonics (in all power spectra plots shown in Figs 8–11 the scale is the same). Higher frequency harmonics are slightly stronger in the non-sinusoidal case. The steady state motion is also supported at slightly lower frequencies to that of the sinusoidal case in both longitudinal and transverse models.

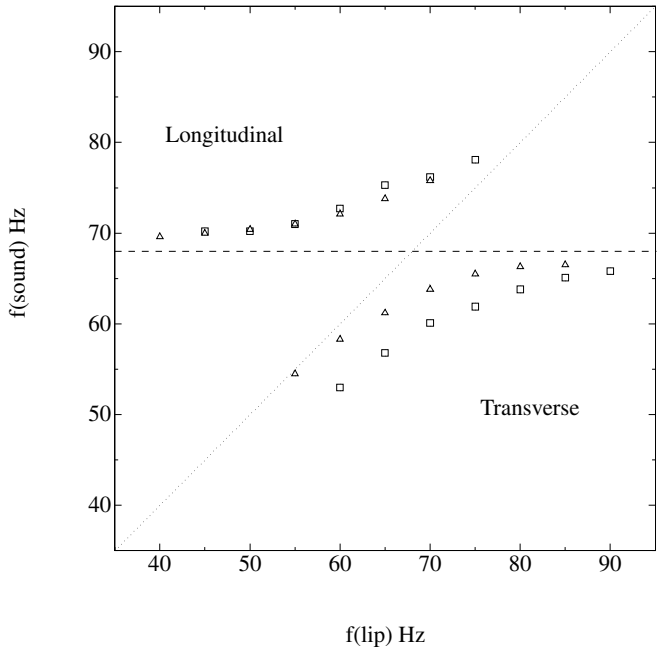

Fig. 12. Summary of sounding frequency versus lip resonance frequency for the simulations shown in Figs 8–11. Sinusoidal cycle results are shown as squares and those of the non-sinusoidal cycle as triangles. The horizontal dashed line is the fundamental resonance for the pipe and the $f_{\text{sound}} = f_{\text{lip}}$ line is shown as a guide.

Again the plot of sounding frequency versus lip resonance frequency shows qualitative agreement with linear theory, even for such an extreme cycle. However, perhaps the most striking feature of the non-sinusoidal cycle results can be seen in Fig. 12—while there is a definite increase in sounding frequency for the non-sinusoidal cycle in the transverse model, there is virtually no change in the longitudinal model. This difference is perhaps due to the fact that the motion in the longitudinal model, with non-zero velocity during closure, has a significant component along the axis of airflow such that, during closure, the acoustic component of the volume flow is dominated by that induced by the lip motion, $b\dot{\theta}/2$.

The possible effect of a sticking collision was studied by enforcing a rapid increase in the Q factor on closure, effectively halting the motion by damping. The universal effect of inducing such a damped cycle was the strangulation of virtually all harmonics resulting in a somewhat unnatural, pure sound wave. This effect occurred in Q-damped cycles for both transverse and longitudinal models. Given that such harmonic suppression is not an observed effect, these observations may be indicative of the importance of the combined motion of the lips during closure.

6. Conclusion

The work presented here represents a first step towards a realistic time-domain simulation of the didjeridu. Low frequency harmonic generation was studied for both sinusoidal and non-sinusoidal lip area functions. In working towards a more complete treatment and

understanding of the dynamic acoustics of this instrument, several significant improvements must be made. To model in more detail a non-sinusoidal lip cycle with relatively large closure times, the one-dimensional models employed here should be extended to two dimensions (Adachi and Sato 1996). Such calculations, with an even larger parameter space than presented here, should only be carried out with quantitative guidance from a comprehensive stroboscopic analysis (as reported in Copley and Strong 1996 for the trombone), and measurements of blowing pressure (as reported in Fletcher and Tarnopolsky 1999 for the trumpet). Given the low frequency domain of lip oscillation, it may transpire that a two-mass lip model might be more appropriate in analogy with vocal-fold motion at low frequency (Ishizaka and Flanagan 1972).

Once the lip dynamics are better understood, the next important component of the sound production system can be included, namely the coupling to the vocal tract, which gives rise to broad and relatively strong formants in the spectrum starting at about 1500 Hz. Such calculations would involve the introduction of a variable volume vocal tract cavity coupled to the valve/pipe system, operating at its half-closed cycle, in order to mimic the many ways the vocal tract is changed during play.

Acknowledgments

I would like to thank Professor Neville Fletcher for many valuable suggestions and comments and a careful reading of the manuscript. Thanks also to A. Rawlinson, D. Bardos, J. Oates, L. Collodetti, and M. Livett. This project was supported by the Australian Research Council, and the Alexander von Humboldt Foundation.

References

Adachi, S., and Sato, M. (1995). *J. Acoust. Soc. Am.* **97**, 3850.
Adachi, S., and Sato, M. (1996). *J. Acoust. Soc. Am.* **99**, 1200.
Chen, F.-C., and Weinreich, G. (1996). *J. Acoust. Soc. Am.* **99**, 1227.
Copley, D. C., and Strong, W. J. (1996). *J. Acoust. Soc. Am.* **99**, 1219.
Fletcher, N. H. (1983). *Aust. Aboriginal Studies* **1**, 28.
Fletcher, N. H. (1993). *J. Acoust. Soc. Am.* **93**, 2172.
Fletcher, N. H. (1996). *Acoustics Aust.* **24**, 11.
Fletcher, N. H., and Tarnopolsky, A. (1999). *J. Acoust. Soc. Am.* **105**, 874.
Ishizaka, K., and Flanagan, J. L. (1972). *Bell System Tech. J.* **51**, 1233.
Jones, T. A. (1967). *Studies in Music* **1**, 23.
Pratt, R. L., Elliott, S. J., and Bowsher, J. M. (1977). *Acustica* **38**, 236.
Schumacher, R. T. (1981). *Acustica* **48**, 71.
Wiggins, G. C. (1985). The Physics of the Didjeridu. BA Thesis, Boston University.
Yoshikawa, S. (1995). *J. Acoust. Soc. Am.* **97**, 1929.

Manuscript received 24 October 2000, accepted 7 February 2001